ENDOR study of Gd3+ complexes in frozen solutions

ARTICLE *in* JOURNAL OF MAGNETIC RESONANCE (1969) · OCTOBER 1986

DOI: 10.1016/0022-2364(86)90365-3

2 AUTHORS, INCLUDING:

Marvin William Makinen
University of Chicago
95 PUBLICATIONS **2,106** CITATIONS

JOURNAL OF MAGNETIC RESONANCE 70, 89–105 (1986)

ENDOR Study of Gd^{3+} Complexes in Frozen Solutions

MOON B. YIM AND MARVIN W. MAKINEN*

Department of Biochemistry and Molecular Biology, The University of Chicago, Cummings Life Science Center, 920 East 58th Street, Chicago, Illinois 60637

Received December 27, 1985; revised April 11, 1986

The coordination environment of Gd^{3+} in frozen solutions is investigated by application of electron nuclear double-resonance spectroscopy. Proton ENDOR spectra of the Gd^{3+} ion in frozen methanol-water cosolvent mixtures obtained with the static laboratory magnetic field (H_0) at the turning point of the electron paramagnetic resonance absorption exhibit single-crystal-type line pairs. With use of selectively deuterated materials, the ligand origin of each pair of ENDOR lines has been assigned. For $GdCl_3$ there are two distinguishable types of protons due to the HO groups of metal-coordinated solvent molecules, and there is one set belonging to the methyl group of metal-coordinated methanol. Similarly, for $Gd(CH_3COO)_3$ and $Gd(CH_3CH_2COO)_3$, the set of ENDOR lines belonging to the methyl group of acetate and to the methylene group of propionate ligands have been identified. By analysis of the dependence of the ENDOR spectra on H_0, we have determined the values of the principal hyperfine coupling (hfc) components of each of the metal-bound ligands. The hfc components of methyl protons of Gd^{3+}-bound acetate and of the methylene protons of Gd^{3+}-bound propionate exhibit axial symmetry. Under the point-dipole approximation, they yield correspondingly calculated metal-proton distances of 4.53 and 4.42 Å in good agreement with the value of 4.73 Å deduced from crystallographic data for inner sphere coordinated ligands. The hfc components of the HO protons of metal-bound solvent molecules do not exhibit axial symmetry. One set is assigned to inner sphere coordinated H_2O while the other is assigned to outer sphere bound CH_3OH. The metal-proton distances, calculated on the basis of the largest anisotropic hfc components as lower limit estimates, support these structural assignments. Application of ENDOR spectroscopy is made to identify the primary lanthanide binding site in α-chymotrypsin and to demonstrate the accuracy with which this method of analyzing ENDOR can be employed for structural characterization of metal complexes in frozen solutions. Comparison of the proton ENDOR spectrum of Gd^{3+} bound to α-chymotrypsin in frozen D_2O solution to those of $Gd(CH_3COO)_3$ and $Gd(CH_3CH_2COO)_3$ indicates that the lanthanide binding site in the protein includes a glutamate residue rather than an aspartate residue. Identification of this protein residue by ENDOR spectroscopy resolves discussions in the literature about the primary lanthanide binding site of α-chymotrypsin.

INTRODUCTION

Lanthanide ions have been widely used as structural probes in studies of calcium-binding proteins by spectroscopic methods (*1–4*) and are frequently employed for phase determination in X-ray crystallographic studies of proteins (*5*). Electron nuclear double resonance is a particularly incisive method for accurate determination of proton positions in single crystals of lanthanide complexes (*6–8*). However, since studies of

* To whom correspondence should be addressed.

0022-2364/86 $3.00

structure-function relationships of biological macromolecules invariably require characterization of their physical and structural properties in solution, it would be important to evaluate the level of structural accuracy that can be obtained by applying ENDOR to molecules in solution. To this end, the Gd^{3+} ion may be particularly useful because of its long electron spin–lattice relaxation time and nearly isotropic g tensor, and because of the generally small Fermi contact interaction that obtains in coordination complexes of lanthanide ions.

The methodology and theoretical basis of frozen solution ENDOR techniques have been described and have been applied to a variety of transition metal ion complexes and organic free radicals to obtain single-crystal-type ENDOR spectra equivalent to those observed for oriented single crystals (*9–12*). However, to date there has been no report of ENDOR studies of Gd^{3+} complexes in frozen solution that can be used as models for application to protein studies. In this communication we present results of an ENDOR study of $GdCl_3$, $Gd(CH_3COO)_3$, and $Gd(CH_3CH_2COO)_3$ in frozen aqueous methanol cosolvent mixtures.[1] By analyzing the static magnetic field dependence of the ENDOR spectra, we show that the hyperfine coupling (hfc) components of the ligand protons yield accurate estimates of metal-proton distances. Furthermore, we apply this methodology to resolve ambiguities that have appeared in the literature (*14–16*) with respect to assignment of the primary lanthanide ion binding site in α-chymotrypsin.

EXPERIMENTAL METHODS

Gadolinium oxide was purchased from Research Chemicals (Phoenix, Ariz. 85063); "Ultrex" HCl from J. T. Baker Chemical Co. (Phillipsburg, N.J. 08865); NaOD (99 at.% D) from Norell, Inc. (Landisville, N.J. 08326); and sodium propionate, D_2O (>99%), and DCl (>99%) from Aldrich Chemical Co. (Milwaukee, Wis. 53201). The deuterated compounds CD_3COOD (99.5%), CH_3COOD (98%), CD_3COOH (99%), CD_3OD (99%), CD_3OH (99%), and CH_3OD (99%) were obtained from Merck, Sharpe & Dohme Isotopes (Montreal, Quebec, Canada). Bovine pancreatic α-chymotrypsin (EC 3.4.4.5; 3 × crystallized and lyophilized) was purchased from Worthington Biochemical Corporation (Freehold, N.J. 07728). All chemicals were used without further purification.

Stock solutions of aqueous Gd^{3+} complexes (1×10^{-3} M) were prepared according to the method used by Marinetti *et al.* (*17*). Concentrations of stock Gd^{3+} solutions were determined by EDTA complexometric titration using xylenol orange (Aldrich Chemical Co.) as the end-point indicator in pH 6 acetate buffer (*18*). The stock solutions were adjusted with NaOH or NaOD to pH 2 for aqueous gadolinium chloride and to pH 6 for aqueous gadolinium acetate and gadolinium propionate. For EPR and ENDOR studies, the final metal ion concentration was 3×10^{-4} M in a 70:30 (v/v) methanol-water cosolvent mixture.

[1] The complexes designated as $GdCl_3$, $Gd(CH_3COO)_3$, and $Gd(CH_3CH_2COO)_3$ are not purported to suggest the exact stoichiometry of the complexes in a solvent mixture, but rather indicate the composition in solid form. For instance, Couture and Rajnak (*13*) have suggested that the coordination polyhedron of the Gd^{3+} ion in frozen H_2O/HCl solution consists only of water molecules.

Stock solutions of α-chymotrypsin were prepared by dissolving the lyophilized protein in solutions of D_2O containing 0.5 *M* NaCl. The nominal pH, as determined with a glass electrode, was ~4 and remained stable upon addition of Gd^{3+}. This procedure was employed to avoid the formation of metal ion complexes with buffer anions. The enzyme was exhaustively dialyzed to ensure absence of possible small peptides and other molecules that could chelate added Gd^{3+}. In addition, information provided by Worthington Biochemical Corporation showed that acetate and propionate buffers are not introduced during enzyme purification. The concentration of protein was based on determination of active sites (*19*). Solutions of Gd^{3+} bound to α-chymotrypsin were prepared by addition of aliquots of aqueous solutions of $GdCl_3$ to the solubilized enzyme in D_2O at pD 4 with monitoring and adjustment of the pD if necessary. The protein was in large excess to ensure >85% complexation of the Gd^{3+} ion, as evaluated on the basis of the binding constants of Ca^{2+} and Tb^{3+} to free α-chymotrypsin (*20*). Proton ENDOR spectra, in general, could be collected with only low signal-to-noise ratios for Gd^{3+} complexes in purely aqueous frozen media. This circumstance could be avoided with use of organic-aqueous cosolvent mixtures, of which aqueous methanol proved to be optimal. On the other hand, for the high protein concentrations required in these studies, methanol could not be employed as a cosolvent because of its tendency to precipitate the enzyme. Although the proton ENDOR signals were relatively weaker for the Gd^{3+}-protein complex than for the small molecule Gd^{3+} complexes in aqueous methanol, adequate spectral resolution was obtained to identify ENDOR line pairs of protons characteristic of the metal ion binding site.

EPR and ENDOR spectra were recorded with a Bruker ER200D spectrometer equipped with an Oxford Instruments ESR10 liquid helium cryostat and a Bruker Digital ENDOR unit. The Bruker broadband ENDOR cavity was operated in the TM_{110} mode. The rf source was a Wavetek signal generator (Model 3000, Wavetek Indiana, Inc., Beech Grove, Ind. 46107) fed into an rf power amplifier (Model 3100L, Electronic Navigation Industries, Inc., Rochester, N.Y. 14623). The rf field is introduced by a silver wire helix (14 turns) mounted directly onto the quartz dewar insert of the Oxford Instruments ESR10 cryostat. ENDOR spectra are presented in the first derivative mode with frequency modulation. Calibration of the sample temperature has been described previously (*21*). Typical conditions for recording ENDOR spectra were: temperature, 5 K; microwave frequency, 9.46 GHz with 12.5 kHz frequency modulation; microwave power, 1.92 mW; rf power, 100 W; modulation depth, 40–90 kHz. No modulation of the static magnetic field was used for recording ENDOR spectra.

RESULTS AND DISCUSSION

A. EPR Characterization of gadolinium complexes. The ground state of $Gd^{3+}(4f^7)$ is $^8S_{7/2}$. In a crystalline field, the eightfold degeneracy is lifted resulting in four Kramers doublets. Therefore, seven $\Delta M = \pm 1$ EPR transitions will be observed for a given general direction of $\mathbf{H}_0$. These transitions are designated $-\frac{7}{2} \leftrightarrow -\frac{5}{2}$, $-\frac{5}{2} \leftrightarrow -\frac{3}{2}$, . . . , $+\frac{5}{2} \leftrightarrow +\frac{7}{2}$.

In Fig. 1 are illustrated the (first derivative) EPR absorption spectra of $GdCl_3$ and $Gd(CH_3COO)_3$ in a 70:30 methanol-water cosolvent mixture. The spectrum of $GdCl_3$

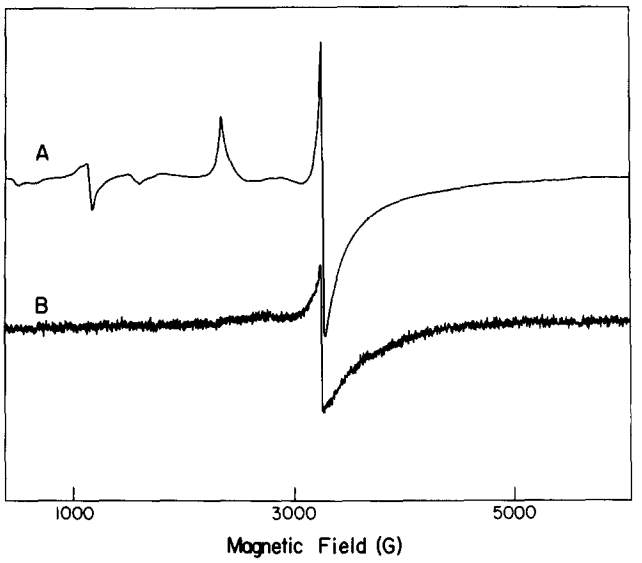

FIG. 1. First derivative EPR absorption spectra of (A) $GdCl_3$ and (B) $Gd(CH_3COO)_3$ in 70:30 (v/v) CH_3OH/H_2O solvent mixtures. The X-band spectra were recorded as described under Methods with the samples at 10 K and with 1.92 mW incident microwave power. The field modulation amplitude was 2.5 G_{pp}. Essentially identical EPR spectra were obtained for samples prepared with selectively deuterated materials.

exhibits a number of low-field resonance lines with the predominant absorption intensity centered near $g \sim 1.99$. To within experimental error, the relative amplitudes of the low-field lines to that at $g \sim 1.99$ remained constant upon dilution of the solution by a factor of 1:50, indicating that none of the resonance lines was due to metal ion clusters. Single crystal studies of Gd^{3+} doped into hydrated rare-earth chlorides (*22, 23*) show spectra corresponding to seven $\Delta M = \pm 1$ transitions, as expected. On the basis of the single-crystal studies, we conclude that the prominant resonance line at $g \sim 1.99$ corresponds to the $+\frac{1}{2} \leftrightarrow -\frac{1}{2}$ transition, the low-field features arising from overlapping effects of other specific EPR transitions that are stationary with respect to the orientation angles of the applied field $\mathbf{H}_0$ over a wide range. This is consistent with the recent analysis of Brodbeck and Iton (*24*) of the EPR spectrum of Gd^{3+} in glasses. In contrast, the EPR spectrum of $Gd(CH_3COO)_3$ in the frozen solvent mixture at pH 6 exhibits only one absorption feature centered near $g \sim 1.99$, the low-field features being presumably too weak or too broad for adequate detection. The EPR spectrum of $Gd(CH_3CH_2COO)_3$ was identical to that of the acetate complex. The lineshape of the $g \sim 1.99$ absorption in both spectra exhibited anisotropy with an apparent peak-to-peak derivative width of ~25 G. The EPR spectrum of the α-chymotrypsin–Gd^{3+} complex was essentially identical to those of $Gd(CH_3COO)_3$ and $Gd(CH_3CH_2COO)_3$.

B. Proton ENDOR and assignment of coordinating ligands by deuterium substitution. The EPR spectra of polycrystalline or amorphous samples are comprised of an average of all molecular orientations with respect to the applied static magnetic field $\mathbf{H}_0$, and such "powder" spectra are described in terms of the anisotropy of the

g and hf tensors. A turning point occurs, in general, at $\mathbf{H}_0$ where one component of the g or hf tensor dominates, and single-crystal type ENDOR spectra can be obtained by setting $\mathbf{H}_0$ at turning points in EPR powder spectra where g or hfc anisotropy is evident (*9–11*). The larger the anisotropy, the better resolved is the selection of a given orientation of the paramagnetic species. This circumstance occurs, for example, for VO^{2+} complexes where the g anisotropy dominates the EPR spectrum and single-crystal-type ENDOR spectra can be easily obtained for the $g_{\|}$ and $g_{\perp}$ orientations (*25–28*). In the case of Gd^{3+} complexes, it has been shown by single crystal studies that the g tensor is nearly isotropic with principal values ranging from 1.991 to 1.993 (*6–8*). On this basis, the anisotropy observed in the broadened EPR spectrum of Gd^{3+} complexes in frozen solutions must originate primarily from the anisotropic hfc interactions of the ligands.

In the general case, the ligand nuclear hf tensor can have any symmetry or orientation, and its axes are not necessarily coincident with those of the g tensor. The resonant frequency of a nucleus will be a complicated function of the direction and magnitude of $\mathbf{H}_0$ and of the g tensor. However, it may be expected that the ligand hf tensor will exhibit only small deviations from axial symmetry under the condition that g anisotropy is small in comparison to the average g value, as is the case for Gd^{3+} (*6–8*). Then the maximum hfc occurs for a field directed along the metal–(ligand) nuclear axis, and the minimum coupling occurs when the field is directed perpendicular to this axis. Because the turning points due to hfc anisotropy are not distinctly identified in the EPR spectra of Gd^{3+} complexes, we have collected ENDOR spectra of complexes in selectively deuterated solvents at a series of $\mathbf{H}_0$ settings to monitor variations in ENDOR spectra and to identify maximum and minimum ENDOR shifts for each type of ligand proton. From the appearance and disappearance of line-pairs in the spectra, we have assigned the hfc components of each type of ligand proton. By identifying the maximum and minimum ENDOR shifts for each type of ligand proton as a function of $\mathbf{H}_0$ setting, we have assumed that Eq. [1]

$$\nu_{\pm} = \nu_{\mathrm{p}} \pm A_{ii}/2 \qquad [1]$$

can be then applied directly for analysis. In Eq. [1] $\nu_{\pm}$ represents the spacing of a single line-pair symmetric about the free proton frequency ν_{p} with $\mathbf{H}_0$ applied parallel to the principal axis i of the proton hf tensor, and A_{ii} represents the corresponding principal component of the hf tensor of the ligand proton.[2]

Figure 2 shows proton ENDOR spectra of $GdCl_3$ obtained at 5 K and with $\mathbf{H}_0$ at the turning point of the EPR absorption. This setting of $\mathbf{H}_0$ maximized the peak-to-peak amplitudes and produced single-crystal-type ENDOR spectra. Spectrum A of $GdCl_3$ in the cosolvent mixture exhibits five pairs of ENDOR lines in addition to the matrix signal centered at the free proton frequency (14.5 MHz). The ENDOR lines in each pair are equally spaced around the free proton frequency and are identified

[2] Recent theoretical analyses of ENDOR shifts from randomly oriented transition metal complexes (*29–31*), that have appeared after submitting this manuscript for publication, show that Eq. [1] holds exactly or very nearly exactly under conditions of low g anisotropy when field orientations correspond to a principal axis of the proton hyperfine tensor. These analyses thus confirm the more qualitative considerations that have guided our analysis of ENDOR spectra of Gd^{3+} complexes in solution.

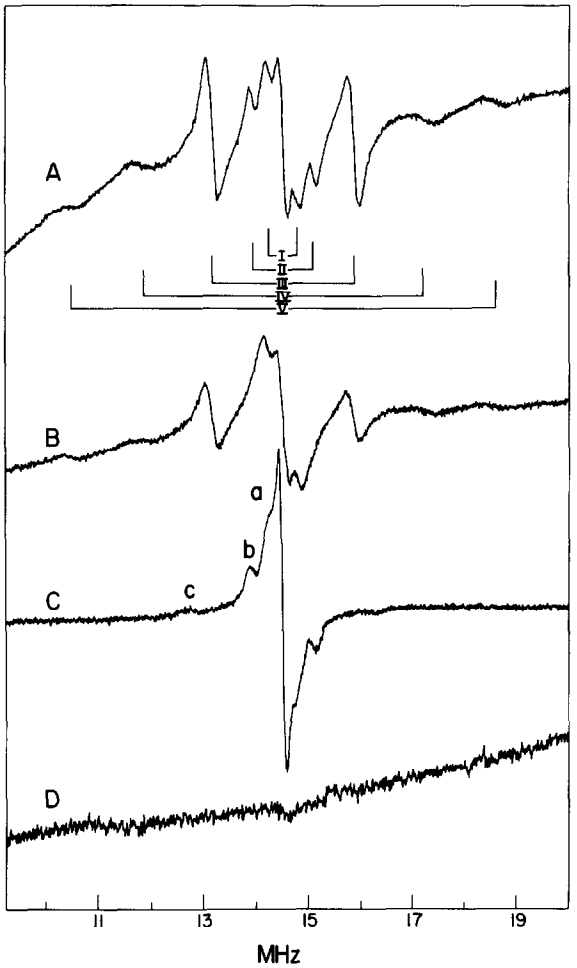

FIG. 2. Proton ENDOR spectra of $GdCl_3$ in 70:30 (v/v) methanol-water solvent mixtures. The samples of $GdCl_3$ were prepared in the following solvent mixtures: (A), CH_3OH/H_2O; (B), CD_3OH/H_2O; (C), CH_3OD/D_2O; and (D), CD_3OD/D_2O. The spectra were collected with H_0 at the turning point of the $g \sim 1.99$ absorption. The single-crystal-type ENDOR lines of each pair are identified in the stick diagram and are seen to be equally spaced about the matrix signal centered at the free proton frequency (14.5 MHz). The line pairs of a and c in spectrum C are not resolved in spectrum A. The line pair of b in spectrum C is identical to II shown in the stick diagram.

in the stick diagram. The corresponding line splittings are listed in Table 1. To identify the ligand origin of each pair of ENDOR lines, solutions of $GdCl_3$ were identically prepared with selectively deuterated materials. In spectrum B, corresponding to $GdCl_3$ in a 70:30 (v/v) CD_3OH/H_2O cosolvent mixture, line pair II is absent while the rest of the line pairs remain, indicating that the other line pairs must belong to metal-bound hydroxyl groups of solvent molecules. Similarly in spectrum C, corresponding to a CH_3OD/D_2O solvent mixture, three pairs of lines are observed.[3] Line pair b

[3] Because exchange of the proton of alcoholic hydroxyl groups with water is relatively rapid (*32*), solvent mixtures cannot be generated in which the methanol hydroxyl group or the water remain selectively deuterated.

TABLE 1

Experimental Data Obtained from Single-Crystal-Type Proton ENDOR Spectra of $GdCl_3$ in Frozen Methanol/Water Cosolvent Mixtures

Line pair[a]	Line splitting[b,c] (MHz)	Linewidth (MHz)	Proton assignment
a	0.460	—[d]	CH_3O-
I	0.526	0.17	$HO_{(2)}$
II, b	1.10	0.17	CH_3O-
II′	1.61	0.17	$HO_{(2)}$
III, III′	2.64	0.23	$HO_{(1)}$ and $HO_{(2)}$
c	3.37	0.28	CH_3O-
IV	5.16	0.45	$HO_{(1)}$
V	7.84	0.45	$HO_{(1)}$

[a] The designation of the labels for each line pair is shown in Figs. 2 and 3.

[b] The ENDOR lines in each pair are equally spaced around the free proton frequency. The line splitting is, thus, twice the value of the ENDOR shift.

[c] The estimated uncertainties of the line splittings are to within ± (linewidth)/2.

[d] The peak-to-peak width of this line pair could not be measured because of overlapping of the matrix line.

identified in spectrum C exhibits an identical ENDOR shift to that of II in spectrum A while the other two, labeled a and c, do not correspond to any line observed in the CH_3OH/H_2O solvent mixture. It is probable, therefore, that line pairs a and c are not resolved in spectrum A because of strong intensity of lines I and III. For the completely deuterated solvent mixture, as shown in spectrum D, all of the ENDOR signals are absent. These observations, thus, identify lines I, III, IV, and V as belonging to protons of hydroxyl groups of methanol or water while lines II, a, and c belong to the methyl protons of methanol.

In Fig. 3 are illustrated ENDOR spectra of $GdCl_3$ in frozen CD_3OH/H_2O solvent at several settings of $\mathbf{H}_0$. With $\mathbf{H}_0$ at the turning point in the spectrum, spectrum A was observed as a single-crystal-type ENDOR spectrum with four line pairs. When $\mathbf{H}_0$ was shifted to higher field, the ENDOR lines of IV broadened and III became much weaker with appearance of a shoulder. With the $\mathbf{H}_0$ setting 50 G higher than the turning point, as shown in spectrum B, shoulder III′ is resolved, indicating that the ENDOR lines III of spectrum A are the superposition of two lines III and III′. A new line pair, II′, between II and III also appeared with the $\mathbf{H}_0$ setting 100 G to higher field from the turning point. Spectrum C illustrates the ENDOR spectrum with the $\mathbf{H}_0$ setting 150 G higher than the turning point. The lines of IV and III′ have disappeared completely, the intensity of I and III have become much weaker than in spectrum A, and the line pair II′ has become more intense.

The following observations can be summarized on the basis of Fig. 3: (i) the maximum number of single-crystal-type line pairs does not exceed six; (ii) the line pairs III′ and IV disappear with $\mathbf{H}_0$ at high field while V remains; and (iii) a new pair, II′, symmetrically located from the free proton frequency appears with $\mathbf{H}_0$ at high field while the intensity of II and III decrease. These results, thus, indicate that two sets of

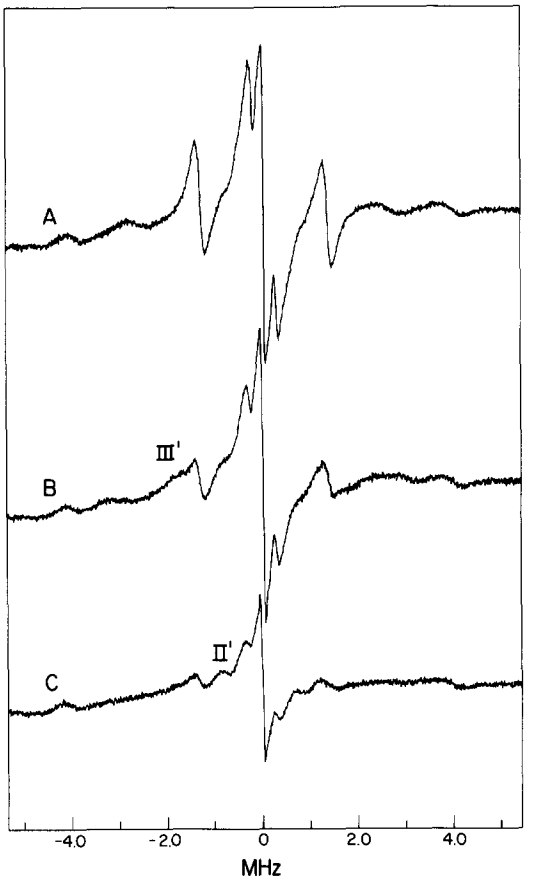

FIG. 3. Proton ENDOR spectra of $GdCl_3$ in a 70:30 (v/v) CD_3OH/H_2O solvent mixture recorded at several H_0 settings. Spectrum A is a single-crystal-type spectrum taken with H_0 at the turning point of the $g \sim 1.99$ absorption. Spectra B and C are recorded with the H_0 setting 50 and 150 G to higher field from the turning point, respectively. Two new line pairs, II' and III', appear at these settings. The horizontal axis represents the ENDOR shift (in MHz) where $\nu = \nu_{observed} - \nu_p$.

hfc components have been observed which can be attributed to two different types of protons of solvent hydroxyl groups. On the basis of these spectra, the experimentally observed hfc components are 7.84, 5.16, 2.64 MHz for one type of hydroxyl proton and 2.64, 1.61, 0.526 MHz for the other type of hydroxyl proton.

For assignment of the ENDOR lines from the methyl protons of methanol, similar experiments were performed. Figure 4 shows the ENDOR spectra of $GdCl_3$ in frozen CH_3OD/D_2O solvent. With H_0 shifted to higher fields from the turning point, the ENDOR signal intensities of a and b decreased continuously while the intensity of c remained almost constant. With the H_0 setting 80 G higher than the turning point, spectrum B was obtained. Above this magnetic field setting, all of the line pairs, a, b, and c, became much weaker and no new lines were observed. We have assigned, therefore, 3.37, 1.10, 0.460 MHz to the experimentally observed hfc components of the methyl protons of methanol.

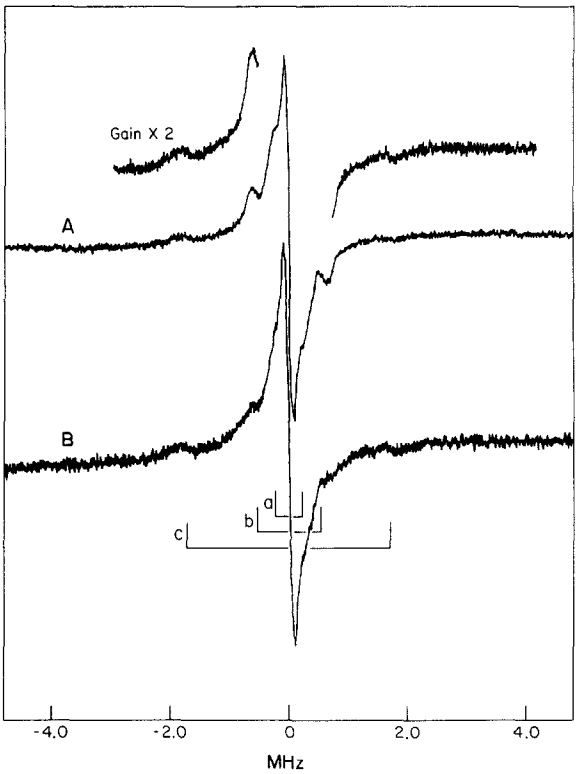

FIG. 4. Proton ENDOR spectra of $GdCl_3$ in a 70:30 (v/v) CH_3OD/D_2O solvent mixture recorded with two different settings of H_0. Spectrum A was taken with H_0 at the turning point. Spectrum B was recorded with the H_0 setting 80 G higher from the turning point and with use of the same gain employed for the partial trace in spectrum A. The stick diagram shows three line pairs due to methyl protons of metal-bound methanol.

Figure 5 shows proton ENDOR spectra of $Gd(CH_3COO)_3$ in selectively deuterated media obtained at 5 K and with H_0 at the turning point of the EPR absorption. In spectrum A, corresponding to $Gd(CH_3COO)_3$ in the CH_3OH/H_2O solvent mixture, six pairs of single-crystal-type ENDOR lines are observed. The ENDOR lines in each pair are equally spaced from the free proton frequency and are identified in the stick diagram. The line splittings are listed in Table 2. In spectrum B, corresponding to $Gd(CD_3COO)_3$ in a CD_3OH/H_2O solvent mixture, the intensity of line pairs I and II decreases, indicating superposition of the ENDOR lines which appear in spectrum A. Therefore, the line pairs observed in spectrum B belong to two different types of protons of solvent hydroxyl groups. Spectrum C obtained with $Gd(CD_3COO)_3$ in a CH_3OD/D_2O solvent mixture exhibits three line pairs, a, b, and c, that belong to the methyl protons of methanol. The frozen solution ENDOR spectrum of $Gd(CH_3COO)_3$ in CD_3OD/D_2O exhibits two pairs of lines, a′ and b′, as shown in spectrum D. These line pairs must belong, therefore, to the methyl protons of acetate.

Figure 6 shows a field dependence study of ENDOR spectra of $Gd(CH_3COO)_3$ in CD_3OD/D_2O solvent mixture. Spectrum A corresponds to spectrum D in Fig. 5. When

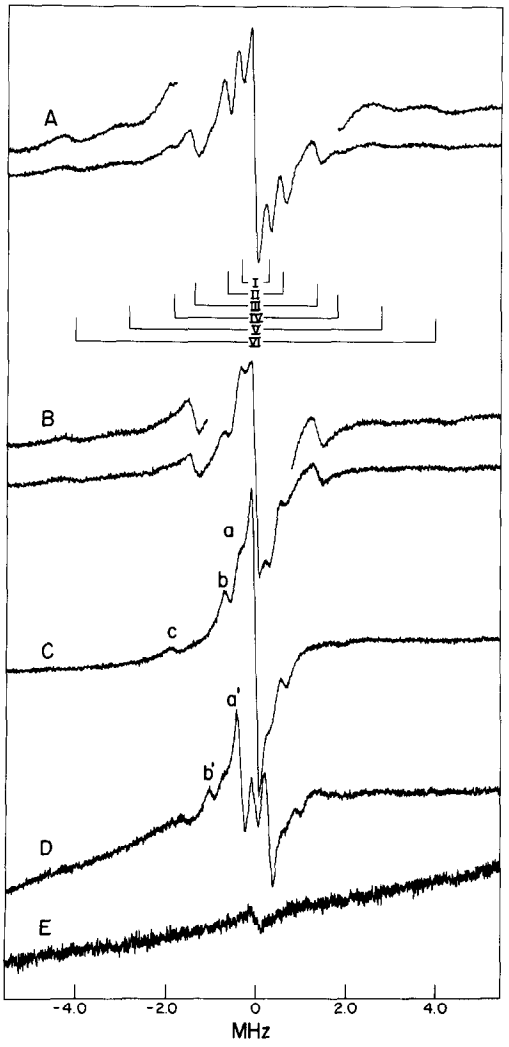

FIG. 5. Proton ENDOR spectra of $Gd(CH_3COO)_3$ in 70:30 (v/v) methanol-water solvent mixtures. (A), $Gd(CH_3COO)_3$ in CH_3OH/H_2O; (B), $Gd(CD_3COO)_3$ in CD_3OH/H_2O; (C), $Gd(CD_3COO)_3$ in CH_3OD/D_2O; (D), $Gd(CH_3COO)_3$ in CD_3OD/D_2O; and (E), $Gd(CD_3COO)_3$ in CD_3OD/D_2O. The spectra were taken with $\mathbf{H}_0$ at the turning point of the EPR spectrum. Six pairs of single-crystal-type ENDOR lines are identified in the stick diagram.

$\mathbf{H}_0$ is shifted to higher field, the intensity of the line pair a′ decreases while that of b′ increases. Spectrum B was obtained at the $\mathbf{H}_0$ setting 150 G higher than the turning point. No new lines are observed. Similar ENDOR spectra and magnetic field dependence behavior were obtained for $Gd(CH_3CH_2COO)_3$ in CD_3OD/D_2O. On the basis of these spectra, the experimentally observed hfc components are 1.87, 0.672, 0.672 MHz for the protons of acetate and 2.08, 0.672, 0.672 MHz for propionate. Magnetic field dependence studies for the protons of solvent hydroxyl groups and for the methyl protons of methanol gave similar results to those described for the $GdCl_3$ system.

TABLE 2

Experimental Data Obtained from Single-Crystal-Type Proton ENDOR Spectra of $Gd(CH_3COO)_3$ in Frozen Methanol/Water Cosolvent Mixtures

Line pair[a]	Line splitting[b] (MHz)	Linewidth (MHz)	Proton assignment
a	0.460	—[c]	CH_3O-
I	0.525	—[c]	$HO_{(2)}$
a′	0.672	0.20	CH_3COO^-
b	1.10	0.16	CH_3O-
II	1.23	0.20	$HO_{(2)}$
b′	1.87	0.20	CH_3COO^-
III	2.96	0.20	$HO_{(2)}$
c	3.37	0.20	CH_3O-
IV	3.70	—[c]	$HO_{(1)}$
V	5.51	0.33	$HO_{(1)}$
VI	7.87	0.33	$HO_{(1)}$

[a] The designation of the labels for each line pair is shown in Fig. 5.

[b] See footnotes *b*, *c* in Table 1.

[c] Peak-to-peak width could not be estimated because of overlapping lines of greater intensity.

C. Estimation of metal–proton distances to assign metal ion coordination structure. Because of the largely noncovalent interactions characteristic of lanthanide ions with their ligand environments, we assume that the experimentally observed ENDOR line splittings listed in Tables 1 and 2 arise predominantly from anisotropic dipolar coupling between the unpaired electron and protons with a smaller contribution from the isotropic Fermi contact interaction. Under the point-dipole approximation and within the strong field limit, the distance between the electron and a nearby proton nucleus can be estimated by

$$A^{\mathrm{D}} = g_e\beta_e g_n\beta_n(3\cos^2\theta - 1)/hr^3. \qquad [2]$$

Here A^{D} is the anisotropic hfc due to the dipole-dipole interaction, r is the modulus of the position vector $\mathbf{r}$ between the nucleus of the metal ion and the proton, and θ is the angle between $\mathbf{r}$ and $\mathbf{H}_0$. To apply Eq. [2] for estimating metal-proton distances, the relative signs of the hfc components have to be determined to identify the anisotropic components. Because of the expected confinement of unpaired electrons to *f* orbitals in lanthanide ions, we have assigned the relative signs of the hfc components so as to give minimum values for the isotropic hfc, as listed in Table 3.

The experimentally observed ENDOR shifts of the acetate and propionate protons reveal axially symmetric hfc components and, therefore, can be straightforwardly evaluated. For the methyl protons of acetate, the isotropic hfc contribution is estimated at 0.18 MHz. We know of no other confirmatory estimate of this interaction for acetate complexes of lanthanides but consider it, in general, reasonable in view of the discussion below. The anisotropic hfc components then derived from the experimentally observed line splittings summarized in Table 3 yield a value of 4.53 Å for the averaged metal-proton distance. With the averaged position of the methyl protons

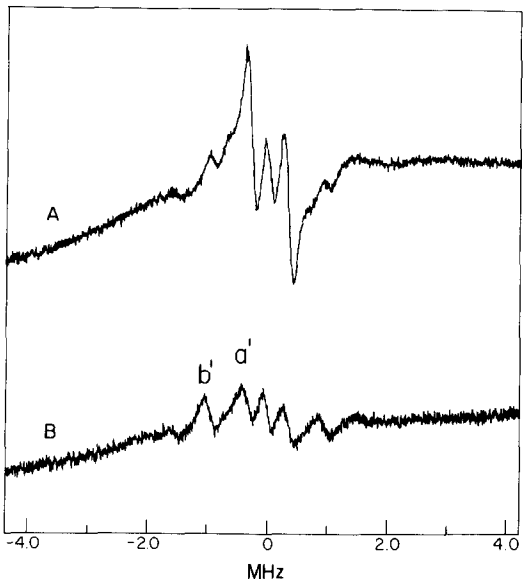

FIG. 6. Proton ENDOR spectra of $Gd(CH_3COO)_3$ in a 70:30 (v/v) CD_3OD/D_2O solvent mixture recorded with two different settings of H_0. Spectra A and B were taken with H_0 at the turning point and 150 G higher than the turning point, respectively. The line pairs of a′ and b′ are due to methyl protons of metal-bound acetate.

taken into account for a tetrahedral carbon and a C–H bond distance of 0.99 Å, the metal-proton distance is estimated as 4.73 Å on the basis of the X-ray-determined bond lengths and bond angles in the crystal of lanthanum nicotinate dihydrate (*33*). The ENDOR result is, thus, in good agreement with that expected on the basis of X-ray data. It is, indeed, possible that the configuration of the metal-bound acetate may differ somewhat from this idealized structure. For instance, highly refined X-ray data of metal-carboxylate interactions show that the metal ion lies slightly out of the plane defined by the carboxylate atoms (*34*). An out-of-plane displacement of only ~0.036 Å, compatible with these observations, would yield a metal-proton separation of precisely 4.53 Å.

The experimentally observed ENDOR line splittings of the propionate protons in the $Gd(CH_3CH_2COO)_3$ complex yield similar estimates of the isotropic and anisotropic hfc components (cf., Table 3), and a metal–proton distance of 4.42 Å is calculated on the basis of Eq. [2]. Since this value is similar to that obtained for the $Gd(CH_3COO)_3$ complex and since no other line pairs were detected that could be attributed to the propionate ligand, we assign these line pairs to the methylene protons. The dipolar contributions of the methyl protons of the propionate ligand estimated for idealized geometries suggests that the ENDOR shifts would be of the order of 0.89 and 0.45 MHz. Since these splittings would be within the detection limits of our experiments, it is probable that these lines are broadened because of the threefold degeneracy in the configuration of the methyl group with respect to the C_1–C_2 bond axis and, therefore, could not be adequately resolved. Although we cannot determine the number of ligands coordinated to the metal ion, these results, nonetheless, demonstrate that for both

TABLE 3

Summary of Proton ENDOR Hyperfine Coupling Components of Gd^{3+} Complexes in Frozen Methanol/Water Cosolvent Mixtures

Complex	Ligand[a]	Isotropic hfc[b] (MHz)	Anisotropic hfc (MHz)		
			A_1	A_2	A_3
$Gd(CH_3COO)_3$	CH_3COO^-	0.175	(1.70	−0.848	−0.848)
	$HO_{(1)}$	−0.447	(8.31	−5.06	−3.25)
	$HO_{(2)}$	0.402	(2.56	−1.63	−0.92)
	CH_3O-	0.604	(2.77	−1.71	−1.06)
$Gd(CH_3CH_2COO)_3$	$CH_3CH_2COO^-$	0.245	(1.84	−0.917	−0.917)
$GdCl_3$	$HO_{(1)}$	0.013	(7.83	−5.17	−2.65)
	$HO_{(2)}$	0.168	(2.47	−1.78	−0.69)
	CH_3O-	0.604	(2.77	−1.71	−1.06)

[a] The abbreviations are CH_3O-, methyl protons of methanol; CH_3COO^-, methyl protons of acetate; $CH_3CH_2COO^-$, methylene protons of propionate; $HO_{(1)}$ and $HO_{(2)}$ designate two different sets of protons of solvent HO groups.

[b] The relative signs of the hfc components are assigned to give minimum isotropic hfc values, as explained in the text.

$Gd(CH_3COO)_3$ and $Gd(CH_3CH_2COO)_3$ in solution anionic acetate and propionate ligands remain coordinated to the Gd^{3+} ion.

To identify other coordinating ligands of isolated $Gd(CH_3COO)_3$, we assign first the origins of the two classes of solvent hydroxyl protons. Later we apply these results to the $GdCl_3$ system. As evident from the experimentally observed ENDOR line pairs, both types of hydroxyl protons do not exhibit axial symmetry, possibly because of aspherical distortion of the closed outer electron shells of Gd^{3+} and spin polarization, as discussed by Freeman and Watson (*35, 36*). The principal hfc components of the metal-bound water protons in gadolinium nicotinate dihydrate determined through a single-crystal ENDOR study similarly exhibit asymmetry (*7*). As noted in Table 3, the two types of solvent HO protons are characterized by isotropic hfc interactions of considerably different magnitude and with different relative sign. For $HO_{(1)}$ the estimated Fermi contact term is approximately −0.45 MHz. This corresponds directly to the averaged Fermi contact term of −0.40 MHz for the protons of the metal-bound water molecules in gadolinium nicotinate dihydrate (*7*). In view of the two similar environments of the Gd^{3+} ion in both complexes with coordinating carboxylate groups, we consequently assign $HO_{(1)}$ to metal-bound water. The anisotropic hfc components evaluated for $HO_{(1)}$ listed in Table 3 yield a metal–proton distance of 2.65–2.90 Å. Despite the approximate nature of such estimates for short electron–nuclear distances, this is in reasonable agreement with the range of metal–proton distances of 2.985–3.195 Å estimated by single-crystal ENDOR techniques in gadolinium nicotinate dihydrate (*7*). Also, for the average Gd^{3+}–OH_2 distance of 2.41 Å determined by X-ray methods for $GdCl_3 \cdot 6H_2O$ (*37*), a metal-proton distance of ~3.0 Å would be expected.

For the second type of solvent HO proton, we estimate an isotropic hfc term of

0.40 MHz. This is distinctly different from that of $HO_{(1)}$ assigned to metal-coordinated water. We believe that this indicates a chemically distinct type of metal-coordinated hydroxyl group that is different from metal-bound water and, therefore, assign $HO_{(2)}$ in Table 3 to Gd^{3+}-bound methanol. While there is, to our knowledge, no direct, confirmatory evidence for lanthanide systems, the isotropic hfc of the methanol HO group evaluated by proton relaxation enhancement of mixed methanol–water complexes of Co^{2+} and Ni^{2+} is in the range of 0.61–0.88 MHz (*38, 39*). Since the Fermi contact term may be expected to reflect less covalency in complexes of lanthanide ions, these results are, thus, in substantial agreement with our assignment. Furthermore, the Fermi contact term of the methyl protons of methanol in mixed methanol–water complexes of Co^{2+} and Ni^{2+} is in the range of 0.39–0.79 MHz (*38, 39*). This is in agreement with our estimate of 0.60 MHz for the isotropic hfc of the methyl protons of metal-bound methanol in Table 3.

The nonaxially symmetric pattern of the principal hfc components evaluated for the HO and the methyl protons of methanol in Table 3 allow only approximate estimates of metal–proton distances on the basis of Eq. [2]. For the HO proton of methanol, the averaged metal–proton distance is estimated at ~3.9 Å, and for the methyl protons a range of 3.6–4.2 Å is calculated. Very similar values for Co^{2+}–methanol interactions in aqueous media were obtained by Luz and Meiboom (*39*). These values suggest that the methanol is outer sphere coordinated with a metal–oxygen interaction of 3.1 Å since the averaged Gd^{3+}–O interaction of the (inner sphere coordinated) hydroxyl group of *tris*(hydroxyacetate)Gd(III) is 2.47 Å (*40*). Although we cannot assign the configuration of the methanol molecule with greater precision, presumably the binding of methanol may be further stabilized through hydrogen bonding interactions with metal-coordinated water molecules or acetate groups.

In general, it would be expected that the isotropic hfc of an outer sphere coordinated ligand is smaller than that of an inner sphere coordinated ligand. The magnitude of the isotropic hfc of the hydroxyl protons assigned to methanol is larger than that of inner sphere coordinated water, as shown in Table 3. This assignment, thus, implies that the mechanism of charge-transfer must be different between the metal ion and methanol molecule to result in more effective spin delocalization than for the direct through bond interaction between the Gd^{3+} ion and a water molecule. We have no further explanation of these observations except to note that similar results are obtained for mixed methanol–water complexes of Co^{2+} and Ni^{2+} (*38, 39*).

In the $GdCl_3$ system the hfc components of the methyl protons of methanol listed in Table 3 are very similar to those observed in the solvated $Gd(CH_3COO)_3$ complex and, therefore, require no further discussion. Also, since the hfc components of $HO_{(2)}$ are essentially identical to those of the methanol HO protons in the $Gd(CH_3COO)_3$ system, we similarly assign $HO_{(2)}$ to the (outer sphere) metal-bound HO group of methanol. The hfc characteristics of $HO_{(1)}$ show a smaller isotropic contribution for solvated $GdCl_3$ than for $Gd(CH_3COO)_3$ with opposite sign to that of metal-coordinated water in the $Gd(CH_3COO)_3$ complex. This difference may indicate a change in the orbital interactions responsible for isotropic hfc from those in the $Gd(CH_3COO)_3$ complex, probably since in this case the coordination polyhedron may comprise only water molecules (*13*). The corresponding hfc components yield estimates for metal–

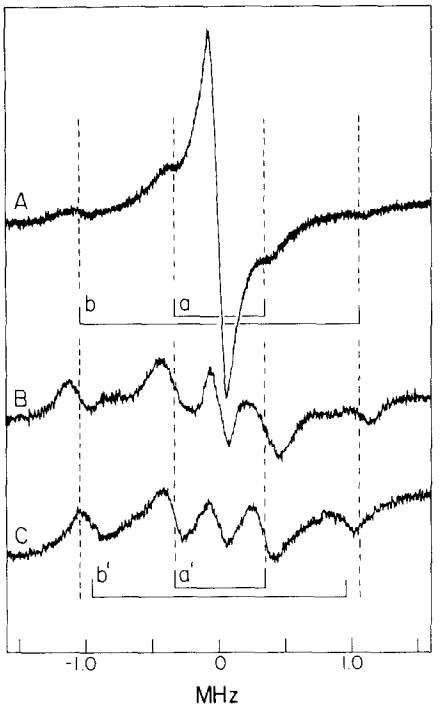

FIG. 7. Comparison of the proton ENDOR spectrum of the α-chymotrypsin-Gd^{3+} complex (spectrum A) to those of $Gd(CH_3CH_2COO)_3$ (spectrum B) and $Gd(CH_3COO)_3$ (spectrum C). To prepare samples for ENDOR spectroscopy, α-chymotryposin was dissolved in D_2O containing 0.5 *M* NaCl, and the nominal pH was adjusted to 4. After centrifugation to ensure optical clarity for determination of protein concentration, the enzyme solution was mixed with a small aliquot of $GdCl_3$ (pH ~ 2). The pH of the resulting mixture was adjusted if necessary to 4 and the solution was examined to ensure the absence of precipitate. The final concentration of protein and metal ion were 5×10^{-3} and 2×10^{-4} *M*, respectively. For spectrum A, the H_0 setting was shifted 150 G to higher fields from the $g \sim 1.99$ turning point at which both line pairs a and b were observed. Spectrum B corresponds to the spectrum of $Gd(CH_3CH_2COO)_3$ in 70:30 (v/v) CD_3OD/D_2O similarly obtained with the H_0 setting 150 G higher than the turning point. Spectrum C corresponds to spectrum B in Fig. 6.

proton distances of 2.5–3.1 Å, as in the solvated $Gd(CH_3COO)_3$ complex, indicating that the metal-bound water is an inner sphere ligand.

D. Assignment of the primary lanthanide ion binding site of α-chymotrypsin. A Ca^{2+} ion required for the conversion of trypsinogen to trypsin binds at a site in the protein that includes the side chains of glutamate-70 and glutamate-80 as ligands (*41*). This site apparently can be occupied also by lanthanide ions (*16*). According to the sequence homology of serine proteases, it would be expected that the primary lanthanide binding site of α-chymotrypsin would also include the corresponding amino acid side chains as ligands. However, Darnall and coworkers (*14, 15*) have assigned the primary lanthanide binding site of α-chymotrypsin to the side chains of aspartate-194 and serine-190 on the basis of fluorescence energy transfer and relaxation enhancement studies, using nuclear magnetic resonance methods. No glutamate side

chain is within coordinating distance in this region of the enzyme. Since the geometries of the side chains of aspartate and glutamate residues should resemble those of acetate and propionate, respectively, we have investigated the ENDOR spectral properties of the complex of Gd^{3+} with α-chymotrypsin to resolve these ambiguities.

Figure 7 compares the proton ENDOR spectrum of the α-chymotrypsin–Gd^{3+} complex in D_2O to those of the $Gd(CH_3COO)_3$ and $Gd(CH_3CH_2COO)_3$ complexes. With $\mathbf{H}_0$ at the turning point of the EPR absorption line, only the line pair a was observed in addition to the strong matrix signal. With an $\mathbf{H}_0$ setting shifted 150 G to higher field, the intensity of the line pair a decreases while the line pair b appears. Identical results were obtained with enzyme exhaustively dialyzed against D_2O for replacement of exchangeable protons by deuterons. The stick diagrams in Fig. 7 correspond to the line splittings observed for the methylene protons of Gd^{3+}-bound propionate (a, b) and for the methyl protons observed for Gd^{3+}-bound acetate (a′, b′). This comparison shows that the splitting of the outer line pair of the α-chymotrypsin–Gd^{3+} complex is identical to that of the $Gd(CH_3CH_2COO)_3$ complex and differs detectably from that of $Gd(CH_3COO)_3$. This result indicates that the Gd^{3+} ion in the enzyme complex is coordinated to amino acid side chain residues of which the molecular properties are essentially identical to those of metal-bound propionate. We conclude, therefore, that the primary lanthanide ion binding site in α-chymotrypsin contains a glutamate residue rather than an aspartate residue. Our results are generally consistent with the sequence homology of the serine proteases, and both glutamate-70 and glutamate-78 in α-chymotrypsin (*42*) are found in environments with secondary structural features similar to those of glutamate-70 and glutamate-80 in trypsin (*41*). Furthermore, Epstein *et al.* (*16*) have pointed out reasons why the relaxation enhancement results of Darnell and co-workers (*14, 15*) probably reflect primarily the influence of a secondary lanthanide binding site.

ACKNOWLEDGMENTS

We thank Mr. G. B. Wells for assistance in titration of enzyme active sites, Professor Clyde A. Hutchison, Jr. for a preprint of Ref. (*7*) prior to publication, and Professor Brian M. Hoffman for helpful discussions. This work was supported by a grant from the National Institutes of Health (GM 21900).

REFERENCES

1. D. W. DARNALL AND E. R. BIRNBAUM, *J. Biol. Chem.* **245,** 6484 (1970).
2. W. DEW. HORROCKS, JR., *in* "Advances in Inorganic Biochemistry" (G. L. Eichhorn and L. G. Marzilli, eds.), Vol. 4, pp. 201–261, Elsevier Biochemical, New York, 1982.
3. R. J. P. WILLIAMS, *Quart. Rev.* **24,** 331 (1970).
4. J. REUBEN, *Biochemistry* **10,** 2834 (1971).
5. T. L. BLUNDELL AND L. N. JOHNSON, "Protein Crystallography," Chap. 8, pp. 183–239, Academic Press, New York, 1976.
6. C. A. HUTCHISON, JR., AND D. B. MCKAY, *J. Chem. Phys.* **66,** 3311 (1977).
7. R. A. FIELDS AND C. A. HUTCHISON, JR., *J. Chem. Phys.* **82,** 1712 (1985).
8. R. DE BEER, F. BIESBOER, AND D. VAN ORMONDT, *Physica* **B83,** 314 (1976).
9. J. S. HYDE, G. H. RIST, AND L. G. G. ERIKSON, *J. Phys. Chem.* **72,** 4269 (1968).
10. G. H. RIST AND J. S. HYDE, *J. Chem. Phys.* **52,** 4633 (1970).
11. R. D. ALLENDOERFER, *Chem. Phys. Lett.* **17,** 172 (1972).
12. B. M. HOFFMAN, J. MARTINSEN, AND R. A. VENTERS, *J. Magn. Reson.* **59,** 110 (1984).

13. L. COUTURE AND K. RAJNAK, *Chem. Phys.* **85,** 315 (1984).
14. F. ABBOTT, J. E. GOMEZ, E. R. BIRNBAUM, AND D. W. DARNALL, *Biochemistry* **14,** 4935 (1975).
15. E. R. BIRNBAUM, F. ABBOTT, J. E. GOMEZ, AND D. W. DARNALL, *Arch. Biochem. Biophys.* **179,** 469 (1977).
16. M. EPSTEIN, J. REUBEN, AND A. LEVITZKI, *Biochemistry* **16,** 2449 (1977).
17. T. D. MARINETTI, G. H. SNYDER, AND B. D. SYKES, *J. Am. Chem. Soc.* **97,** 6562 (1975).
18. S. J. LYLE AND M. RAHMAN, *Talanta* **10,** 1177 (1963).
19. M. L. BENDER, G. R. SCHONBAUM, AND B. ZERNER, *J. Am. Chem. Soc.* **84,** 2540 (1962).
20. J. DE JERSEY, R. S. LAHUE, AND R. B. MARTIN, *Arch. Biochem. Biophys.* **205,** 536 (1980).
21. M. B. YIM, L. C. KUO, AND M. W. MAKINEN, *J. Magn. Reson.* **46,** 247 (1982).
22. M. WEGER AND W. LOW, *Phys. Rev.* **111,** 1526 (1958).
23. S. K. MISRA AND G. R. SHARP, *J. Chem. Phys.* **64,** 2168 (1976).
24. C. M. BRODBECK AND L. E. ITON, *J. Chem. Phys.* **83,** 4285 (1985).
25. H. VAN WILLIGEN, *Chem. Phys. Lett.* **65,** 490 (1979).
26. H. VAN WILLIGEN, *J. Magn. Reson.* **39,** 37 (1980).
27. C. F. MULKS AND H. VAN WILLIGEN, *J. Phys. Chem.* **85,** 1220 (1981).
28. C. F. MULKS AND H. VAN WILLIGEN, *J. Am. Chem. Soc.* **104,** 5906 (1982).
29. G. C. HURST, T. A. HENDERSON, AND R. W. KREILICK, *J. Am. Chem. Soc.* **107,** 7294 (1985).
30. T. A. HENDERSON, G. C. HURST, AND R. W. KREILICK, *J. Am. Chem. Soc.* **107,** 7299 (1985).
31. N. D. YORDANOV, M. ZDRANKOVA, AND D. SHOPOV, *Chem. Phys. Lett.* **124,** 191 (1986).
32. Z. LUZ, D. GILL, AND S. MEIBOOM, *J. Chem. Phys.* **30,** 1540 (1959).
33. J. W. MOORE, M. D. GLICK, AND W. A. BAKER, JR., *J. Am. Chem. Soc.* **94,** 1858 (1972).
34. H. C. FREEMAN, *Adv. Prot. Chem.* **22,** 257 (1967).
35. R. E. WATSON AND A. J. FREEMAN, *Phys. Rev. Lett.* **6,** 277 (1961).
36. A. J. FREEMAN AND R. W. WATSON, *Phys. Rev.* **127,** 2058 (1962).
37. M. MAREZIO, H. A. PLETTINGER, AND W. H. ZACHARIASEN, *Acta Crystallogr.* **14,** 234 (1961).
38. Z. LUZ AND S. MEIBOOM, *J. Chem. Phys.* **40,** 1066 (1964).
39. Z. LUZ AND S. MEIBOOM, *J. Chem. Phys.* **40,** 2686 (1964).
40. I. GRENTHE, *Acta Chem. Scand.* **26,** 1479 (1972).
41. W. BODE AND P. SCHWAGER, *FEBS Lett.* **56,** 139 (1975).
42 D. BLOW, *in* "The Enzymes" (P. Boyer, ed.), Vol. III, pp. 185–212, Academic Press, New York, 1971.